Magnetic resonance detection: spectroscopy and imaging of lab-on-a-chip

Elad Harel

Received 25th April 2008, Accepted 19th August 2008
First published as an Advance Article on the web 16th October 2008
DOI: 10.1039/b807036a

This mini-review is focused on the use of nuclear magnetic resonance (NMR) spectroscopy and imaging to study processes on lab-on-a-chip devices. NMR as an analytical tool is unmatched in its impact across nearly every area of science, from biochemistry and medicine to fundamental chemistry and physics. The controls available to the NMR spectroscopist or imager are vast, allowing for everything from high level structural determination of proteins in solution to detailed contrast imaging of organs *in-vivo*. Unfortunately, the weak nuclear magnetic moment of the nucleus requires that a very large number of spins be present for an inductively detectable signal, making the use of magnetic resonance as a detection modality for microfluidic devices especially challenging. Here we present recent efforts to combat the inherent sensitivity limitation of magnetic resonance for lab-on-a-chip applications. Principles and examples of different approaches are presented that highlight the flexibility and advantages of this type of detection modality.

Introduction

While optical detection is overwhelmingly the method of choice for analysis of fluid transport in microstructured devices,[1] it has some serious limitations. Laser induced fluorescence (LIF), the most sensitive and widely used technique is well suited for naturally fluorescent molecules or for analytes that can be made fluorescent through interaction with a fluor. Unfortunately, most biomolecules and chemical compounds do not conform to this stringent requirement. The most notable restriction of optical methods is the need for optical access to the region of interest which necessarily limits the range of materials that can be used for device fabrication. While one material may work well for UV detection, it may bode poorly for light in the visible or IR region of the spectrum. Secondly, tracers which are typically needed to visualize the fluid flow path can alter the hydrodynamic properties at these small dimensions.[2] Another limitation of optical detection is that the short optical path length through the device makes absorption based spectroscopy such as UV on the chip difficult. Other detection techniques such as IR detection[3] have been reported on microfluidic devices, although generally they can only analyze one point on the device at a time, precluding imaging. Confocal Raman spectroscopy does seem to be a promising approach for spectroscopic imaging in microfluidic devices,[4] although it is typically restricted to analyzing known compounds. Furthermore, long acquisition times do not allow for on-line, time resolved studies needed for many kinetic problems.

Department of Chemistry, University of California, Berkeley, CA, 94720, USA. E-mail: elharel@berkeley.edu; Tel: +1 510 642 2094

Elad Harel *received his BA in Mathematics and BS in Chemical Physics from the University of California, San Diego in 2003, under the supervision of Robert E. Continetti. Harel then went on to receive his PhD at the University of California, Berkeley in Physical Chemistry under the guidance of Alex Pines in the spring of 2008. His research focus at Berkeley was in developing novel detection methods using NMR and MRI as it applies to porous materials and microfluidics. In the fall of 2008, he will start a postdoctoral fellowship at the University of Chicago.*

Magnetic resonance can bypass some of these limitations because of its non-invasiveness and ability to incorporate imaging and spectroscopy simultaneously.[5] Spectroscopic imaging in which a spectrum is acquired for every pixel in the image is routinely practiced in medical imaging applications and is becoming increasingly used for materials characterization.[6] Furthermore, through the incorporation of multidimensional techniques, NMR can elucidate structure and dynamics of large molecules and proteins in solution.[7] For all its prowess, however, the sensitivity of magnetic resonance is noticeably poor compared to most other detection techniques due to the small energies involved even at the highest available magnetic field strengths. This presents itself as a particular challenge in microfluidic applications where picomolar or smaller quantities of analyte are measured. Compounding this problem is the fact that the radio-frequency (RF) excitation and detection must occur over the volume of the entire chip, while only a fraction is occupied by the fluid that gives rise to the NMR signal. For microfluidics the direct sensitivity is less than 10^{-4} of traditional high-resolution NMR under these conditions.

While several methods have been developed to deal with ultra-small-samples such as microsolenoid RF coils for NMR,[8–10] and magnetic resonance force microscopy (MRFM),[11] to name a few, this review is concerned only with those techniques compatible

with conventional planar microfluidic devices of arbitrary channel geometry under standard operating conditions. This requirement limits the discussion to those methods in which any location of the device can be analyzed either spectroscopically or through imaging without making physical contact with the sample such as necessary with force detection. Furthermore, force detection requires very low temperatures not compatible with liquid samples. Microsolenoids, while extremely sensitive, cannot be readily integrated into the device simply due to the incompatibility of geometries and, hence, are outside the scope of this review.

Here we review several methods that overcome the sensitivity limitation of traditional magnetic resonance on lab-on-a-chip. The methods can be grouped into two categories: direct detection and remote detection. The merits and pitfalls of each as well as prospective avenues for future improvements are discussed.

Direct detection

Direct detection refers to the class of experiments were the excitation and detection of the nuclear spins occurs using the same radio-frequency coil, as in conventional NMR.[12] The signal-to-noise of an NMR experiment utilizing inductive detection and assuming uniform sensitivity throughout the sample is given by[13]

$$\mathrm{SNR} = \frac{\gamma(B_1/i)V_s N\eta^2 I(I+1)\omega_0^2}{3\sqrt{2}kT_S V_{\mathrm{noise}}}$$

where γ is the gyromagnetic ratio, (B_1/i) is the magnetic field per unit current generated by the RF coil, V_S is the sample volume, T_S is the sample temperature, N is the number of spins, I is the spin quantum number, ω_0 is the Larmor precession frequency (proportional to the static field strength:$\omega_0 = \gamma B_0$), and

$$V_{\mathrm{noise}} = \sqrt{4kTR_{\mathrm{noise}}\Delta f}$$

R_{noise} is the resistance of the coil plus any other losses due to the RF circuit and Δf is the bandwidth of the receiver. The resistance in turn is dependent on the size of the coil so that the overall signal-to-noise for a solenoid coil is proportional to the filling factor defined as

$$\eta = \frac{V_S}{2V_C}$$

where V_C is the coil volume and the factor of 2 comes from the fact that for a solenoid coil only half of the B_1 field resides within the coil. For other coil geometries, the filling factor will change depending on the profile of $B_1(r)$.

For microfluidics the filling factor is very small since the pickup coil must fit around the entire device which is macroscopic in size, while the fluid which gives rise to the signal is microscopic. For conventional NMR the filling factor is close to 50%, while in microfluidics the filling factor can be lower than 10^{-4}, a loss of four orders of magnitude. For NMR which is already an insensitive technique this hit in signal-to-noise is devastating.

In order to increase the filling factor several groups have fabricated planar microcoils directly on the microfluidic device.[14,15] Although less sensitive than solenoid coils, planar geometries are compatible with planar microfluidic devices and relatively easy to fabricate. These detectors are significantly more sensitive than a large, encompassing coil geometry because they reside very close to the microfluidic channels, increasing the filling factor, and their small size allows for much higher (B_1/i). A schematic of a microcoil fabricated by micro-photolithography on top a microfluidic chip is shown in Fig. 1.

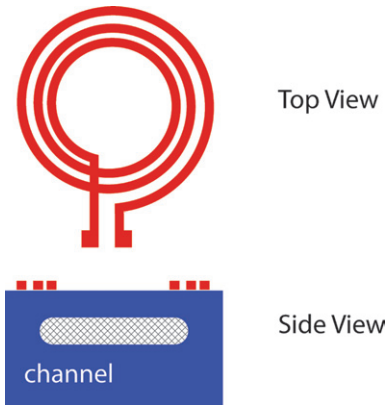

Fig. 1 Schematic of an electroplated planar microcoil integrated on a glass microfluidic device with etched channels.

Several applications of planar microcoils on lab-on-a-chip have been demonstrated. Trumbull *et al.*[16] integrated a planar microcoil on a capillary electrophoresis (CE) chip, demonstarting a linewidth of less than 1.5 Hz of a 30 nL sample of water. Wensink *et al.*[15] measured reaction kinetics of imine formation from benzaldehyde and aniline. Popovic *et al.*[17] recorded spectra of mammalian cells with a sample volume corresponding to as little as 1800 cells. The main factor that limits spectral resolution and hence sensitivity is the static magnetic field inhomogeneities induced by the interfaces of the coil material, microfluidic components, and fluid inside the microchannels.[14] Although planar microcoil fabrication is scalable to smaller dimensions, the signal sensitivity due to this inhomogeneous broadening effect becomes more pronounced. Furthermore, the sensitivity of the planar microcoils falls off as r^{-1}, such that path length effects become noticeable, akin to problems experienced by linear optical techniques. Another approach demonstrated by Maguire *et al.*[18] utilized microslot waveguides, which are planar structures based on a dual-layer, metallic microstrip. These structures are used to transport quasi-transverse electromagnetic mode (TEM) RF signals on dielectric materials. This microslot waveguide, due to its geometry does not have the severe static magnetic field distortions of a planar microcoil, allowing for higher sensitivity. A two dimensional COSY spectrum acquired using the microslot probe is shown in Fig. 2 on ribonuclease-A. While this microslot has not been integrated directly onto a microfluidic device, in principle such a detector could be used due to its planar geometry.

Direct imaging

While planar microcoils provide high resolution NMR spectra directly on the microfluidic device they have two serious drawbacks that make them less attractive for the purposes of imaging. First, due to their relatively large fingerprint only a few planar

This journal is © The Royal Society of Chemistry 2009

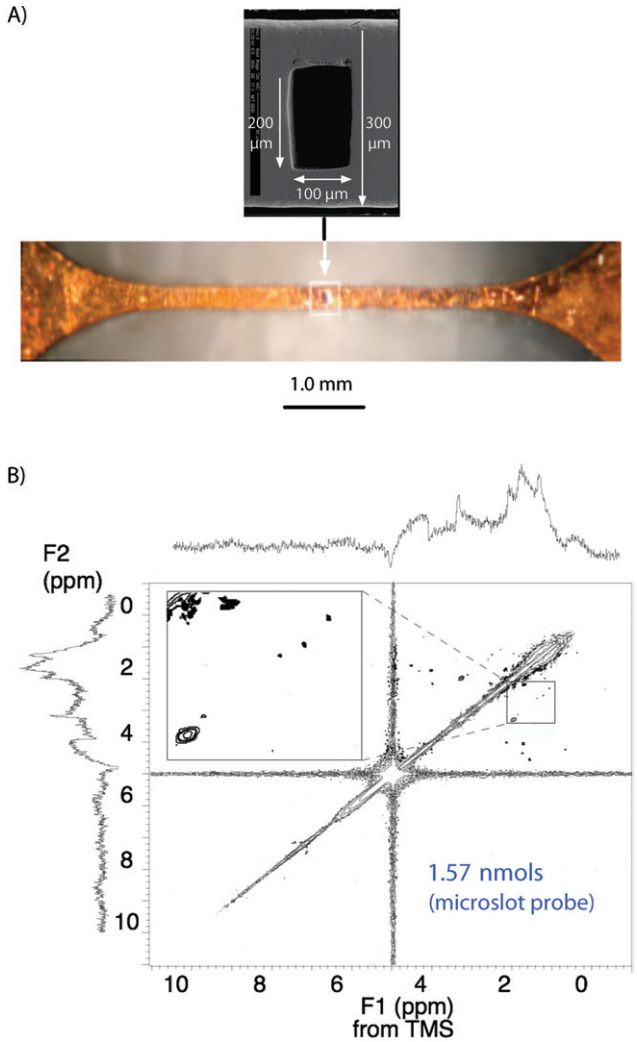

Fig. 2 A. Microslot waveguide fabricated with a 248 nm eximer laser. B. Two-dimensional correlation spectrum (COSY) of ribonuclease-A. Used with permission from ref. 14.

structures can be fabricated on a single device.[19] Even in the case of microslots which have a smaller fingerprint and better ability to pack multiple detectors close together due to weaker inter-structure couplings, integration of parallel detectors is extremely difficult due to the complicated electronics that would be required. Each detector would have to have its own transmitter and receiver channel which would make the technique extremely expensive and impractical. For applications involving reactions or mixing, the chip would have to be designed such that the interaction of interest occurs precisely in the position of the detector. Most importantly, the extra expense and complication of altering already established chip fabrication protocols to accommodate planar microstructures may offset the potential benefits of NMR detection in the first place. Although imaging gradients, could, in principle be used to differentiate channels that are close in space with planar microcoil detection, this would negate to a large degree the advantages of using a small detector.

A few groups have recorded images on microfluidic devices by using large, macroscopic surface coils, even with the poor filling factor problem. NMR microscopy techniques allow the user to control the type of flow property to be measured. While MRI typically detects spin density or relaxation contrast, it is also possible to encode for velocity, acceleration, or diffusion by employing multiple gradients that measure the desired phase while cancelling all other unwanted sources of phase accumulation.[20] Ahola *et al.*[21] monitored fluid motion in a micromixer by measuring the velocity distributions of water at a spatial resolution of 29 µm × 43 µm. Another nice example of this type of approach is the work by Akpa *et al.*[22] using a conventional birdcage RF coil, that measured concentration and flow mapping of immiscible flow inside a low aspect ratio microfluidic device which would otherwise be difficult to study with optical techniques that produce *en face* images. Spin density and velocity maps through a cross-section of the device are shown in Fig. 3.

Remote detection

A completely different approach to the detection of microfluidic devices by NMR, pioneered in the lab of Alex Pines at UC Berkeley, which is known as remote detection takes advantage of the flow inherent in microfluidics, coupled with the long relaxation times of the NMR sensor in order to detect the spin magnetization off the chip with high homogeneity and sensitivity.[23,24] By decoupling the excitation and detection of the MR experiment, it is possible to obtain high sensitivity across the entire microfluidic device irrespective of the coil filling factor.

The remote detection scheme is shown in Fig. 4A. The fluid flows through the microfluidic device which is encased inside a macroscopic RF coil. The nuclear spins of the fluid are initially

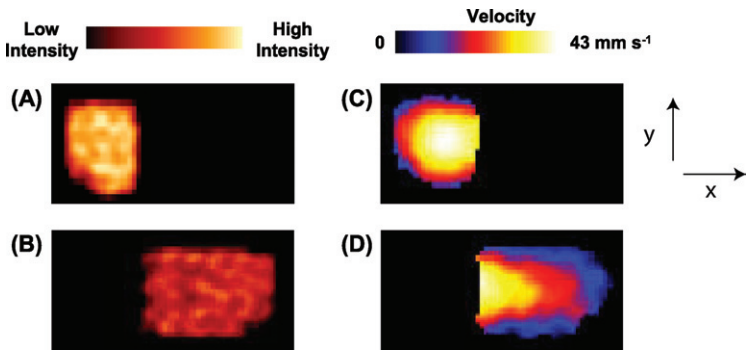

Fig. 3 Cross-sectional images of immiscible flow through a microfluidic channel of two fluids converging. Spin density and velocity maps of oil (A, C) and water (B, D), respectively. Used with permission from ref. 18.

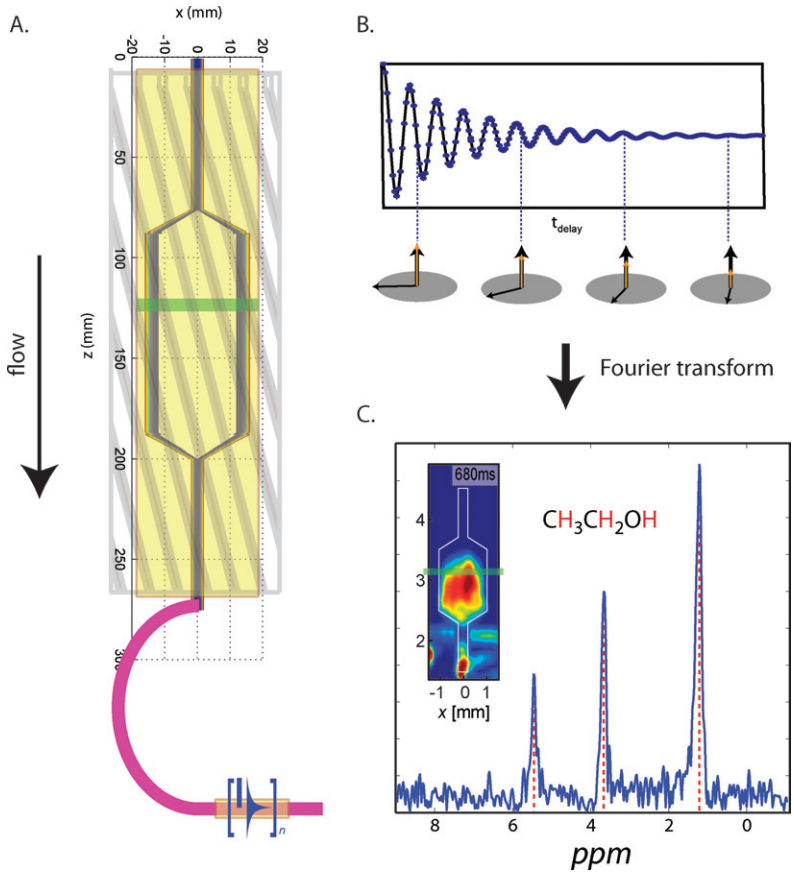

Fig. 4 Remote detection method: A. Spins are excited by an application of a spatially selective RF pulse (green stripe) in the encoding region (grey stripes). The magnetization encodes spectroscopic or imaging information in the form of a complex phase which is 'stored' by application of a broadband RF pulse. B. Each phase incrimination corresponds to one point in the indirect interferogram. C. Upon Fourier transformation the spectrum or image (inset) is formed for each detection pulse.

excited by application of an RF pulse and begin precession into the transverse plane. The phase accumulation can proceed by free evolution (*i.e.* chemical shift) which encodes spectroscopic information or in the presence of gradients which can encode spin density, relaxation weighting, motion, *etc.* At this point the encoding scheme is identical to any other pulse sequence available to NMR or MRI. After adequate phase accumulation the transverse component of the magnetization is 'stored' as longitudinal magnetization by the application of a broadband RF pulse. This is necessary because the longitudinal relaxation of the spins (T_1) is typically much longer than the transverse relaxation time (T_2). The magnitude of the magnetization along the longitudinal direction is a direct indicator of the phase of the spin at the moment the 'storage' pulse was applied (Fig. 4B). This encoding typically occurs very rapidly relative to the time scale of flow such that it can be taken to be instantaneous. The encoded spins then flow to a highly sensitive microsolenoid detector where application of a train of hard pulses reads out the magnitude of the magnetization. Phase cycling is performed to get frequency discrimination (*i.e.* quadrature detection) as well as baseline correction.

Fig. 4C shows an example of ethanol flowing through a single channel microfluidic device. The spectrum of the ethanol can be reconstructed by recording the interferogram of chemical-shift evolution point-by-point and Fourier transforming for each detection pulse. Here, spatial excitation occurs only over a thin slice, meaning that this spectrum corresponds to a specific spatial location on the chip, demonstrating that spectroscopic imaging is indeed possible (see inset for the full image). In addition, to this type of image and spectroscopic reconstruction, remote detection naturally allows the dynamics of the flow to be recorded. Since the detector is typically much smaller than the encoded volume, it takes many separate detection acquisitions to record the entire encoded fluid packet. Since the timing of these pulses is accurately controlled, the time-of-flight (TOF) of the encoded spins can be mapped and an image or spectrum can be formed for each detection pulse. Furthermore, because detection occurs outside the microfluidic device, it is possible to record high resolution spectra in the detector as well, so that even if the homogeneity on the microfluidic chip is too poor to perform high resolution spectroscopy, it is still possible to recover the dynamics of flow for each species. An example of this concept is illustrated in Fig. 5A where the confluence of water and ethanol is imaged through a T-chip device at high spatiotemporal resolution.[25] It is also possible to zoom in on regions of interest by using spatially selective pulses. This shows that the ethanol and water in fact do not mix at the low Reynolds used here for the current mixer geometry.

 This journal is © The Royal Society of Chemistry 2009

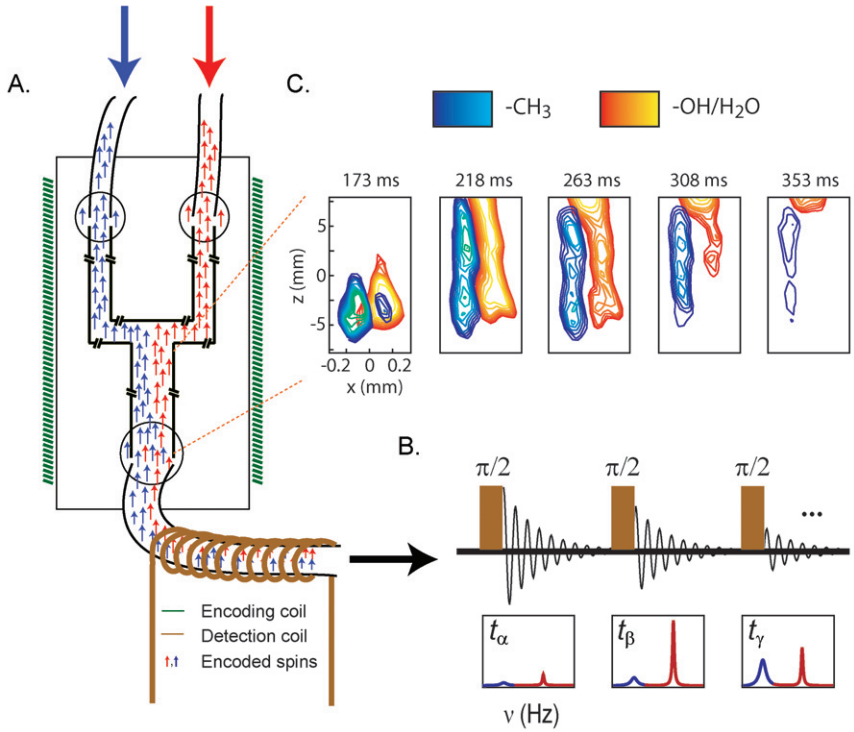

Fig. 5 Schematic of time-of-flight (TOF) imaging of two fluids inside a T-mixing chip (A) based on chemical shift selection in the detector (B). For each detection pulse an image is formed of each species separated by their chemical shift (C).

It is also possible to combine imaging and spectroscopy in the detector as well as to obtain even higher temporal resolution as shown in Fig. 6.[26] This is made possible by recognizing that the spatial dimension in the detection region is related to TOF of encoded spins. By slicing up space, one effectively slices up the time of arrival of the spin packets to a degree determined by the spatial resolution in the detector. Typically, the residence time in the detector determines both the spectral resolution as well as the TOF resolution. However, by recording a spectroscopic image in the detector it is possible to decouple these two dimensions of the experiment, bypassing the common assumption that the time scale of observation of the time variable limits the certainty with which one can measure the spectral dimension. By employing spectroscopic imaging in the detector it is possible to overcome this apparent limit inherent in Fourier pairs, allowing, in principle, for arbitrarily high temporal resolution. The enhancement is evidenced by recording chemically resolved fluid mixing of benzene and acetonitrile at 500 frames per second (2 ms time resolution), the highest recorded in a magnetic resonance imaging experiment.

Comparison of direct and remote detection

The advantages of remote detection are that any microfluidic device can be used as long as it can fit inside the bore of a high-field magnet and as long as fluidic components are compatible with high magnetic fields. However, even in special cases where these conditions are not met it is possible to perform the remote detection experiments at low field and even without inductive detection as shown by Xu *et al.* who used an optical magnetometer to image the flow of water through a phantom.[27] The main advantage is that encoding and detection can be independently optimized. Detection proceeds with a very high filling factor and sensitivity and in a high-homogeneity environment allowing imaging and spectroscopy at spatial and spectral resolutions difficult to achieve with direct detection methods. The main disadvantage of remote detection is the need to perform the experiment in an indirect fashion, causing the total experiment time to be relatively long. However, compared to direct detection which requires signal averaging, this does not scale as poorly as expected. At concentrations of chemical and biological relevance it is unlikely that direct detection can access the small dimensions of microfluidic devices for imaging purposes. However, for spectroscopy, in particular of non-mobile samples such as cells, direct detection is highly advantageous.

Direct detection can also complement remote detection in several ways. For example, the ability to record an image both directly and remotely can give insight into stagnant or recirculating flow. It may also be possible, by placing planar microcoils at the inlets or outlets of the microfluidic device, to label spins with significantly improved efficiency. While labelling spins by a combination of magnetic field gradients and RF pulses is flexible it does have certain practical disadvantages owing to the relatively long pulse durations of large macroscopic, and hence low (B_1/i) RF coils. Labelling spins by inversion or saturation using small planar structures could provide for much faster encoding and attenuation of flow artefacts. Current research along both avenues is proceeding rapidly and the field of NMR on a chip is only a couple of years old. With the advent of commercial hyperpolarization methods it should be possible to substantially increase the sensitivity of both direct and remote detection methods.[28]

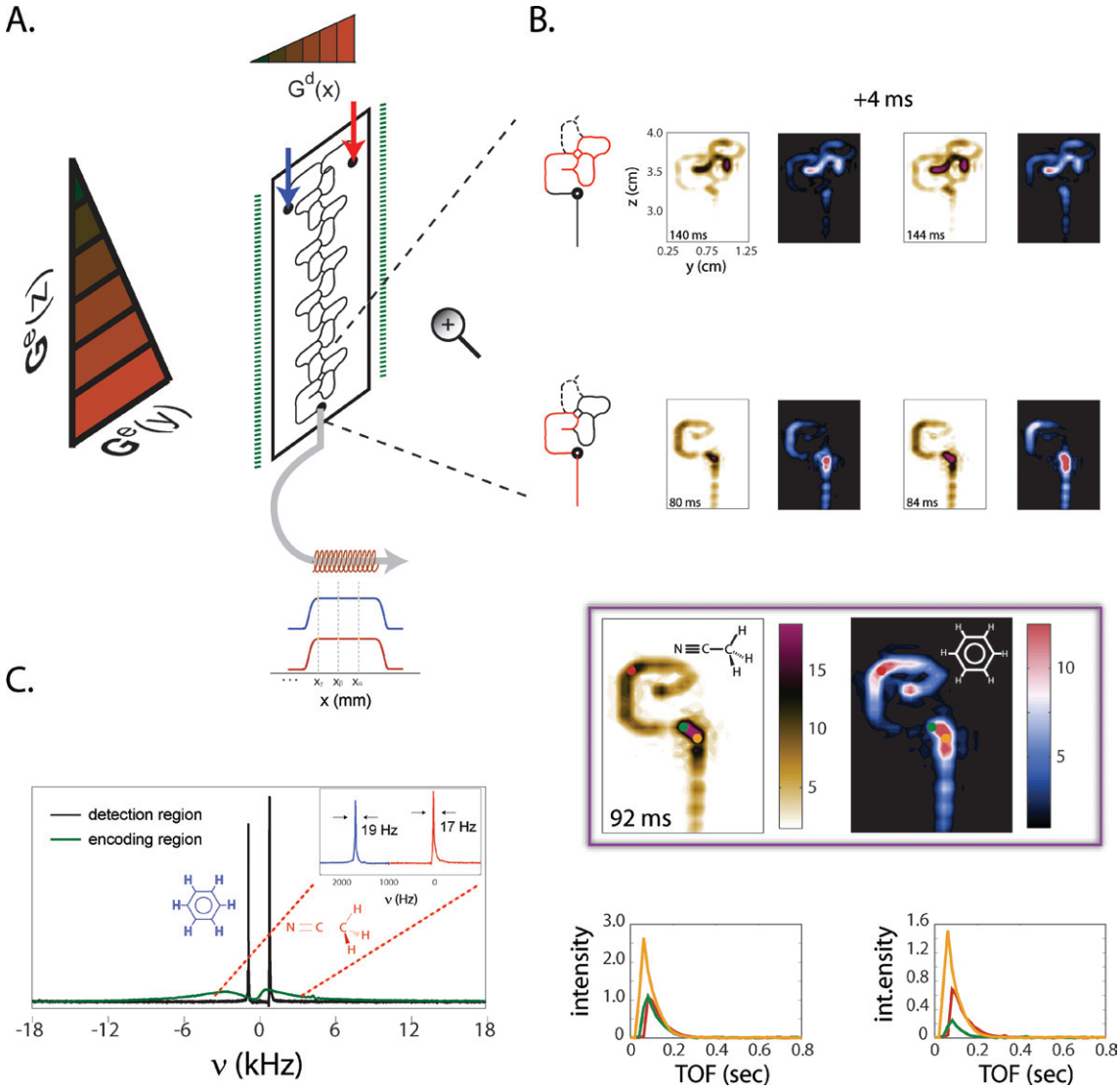

Fig. 6 A. Schematic of remote detection with time slicing of the TOF dimension. A spectroscopic image is formed in the detector, with each position along the 1D profile corresponding to a different TOF value of encoded spins. B. Partial images taken from the integrated data set. For each point in the image a TOF curve is measured which gives information about the time of arrival and dispersion of the encoded fluid voxel. Differences at the outlet (green curve) show that the fluid species begin to separate in the dead volume near the outlet connector. C. Comparison of spectra acquired inside and outside of the chip showing that the resolution off the chip is dramatically improved compared to on the chip.

Conclusions

Detection by NMR opens up the possibility of using a whole new class of materials for microfluidic device fabrication as optical transparency is no longer required. No tracers are used in NMR and due to the noninvasive nature of magnetic resonance, there is never the worry that the hydrodynamic properties of the fluid are somehow altered. While the spatial resolution of magnetic resonance is below that of optical detection, it should be possible to obtain better than 5 μm isotropic resolution which is adequate for most applications. Furthermore, the use of relaxation contrast (*i.e.* T_1 and T_2 weighting) and chemical shift allows differentiation of fluids irrespective of their optical properties. By employing three-dimensional imaging methods, any point on the microfluidic device can be analyzed, unlike most optical methods that are restricted to the *en face* type where the concentration profiles are a projection through the entire depth of the channel. The ability to easily manipulate the spins by application of RF fields allows for a large body of information to be recorded, whether it be fluid mechanics (*e.g.* velocity, acceleration, diffusion) or chemical and physical properties (*e.g.* chemical shift, scalar couplings, correlation spectroscopy, reaction kinetics, dynamics). Future work along the lines of exploiting many of the tools available to MR towards lab-on-a-chip applications promises to be an exciting area of research and development.

Acknowledgements

Discussions, encouragement, and support from Professor Alex Pines is greatly appreciated.

 This journal is © The Royal Society of Chemistry 2009

References

1 S. Devasebathipathy, J. G. Santiago, S. T. Wereley, C. D. Meinhart and K. Takehara, *Exp. Fluids*, 2001, **34**, 504.
2 D. Ross and L. E. Locascio, *Anal. Chem.*, 2003, **75**, 1218.
3 S.-A. Leung, R. F. Winkle, R. C. R. Wootton and A. J. de Mello, *Analyst*, 2005, **5**, 431.
4 F. Sarrazin and J.-B. Salmon, *Anal. Chem.*, 2008, **80**, 1689.
5 H. Rampel and J. M. Pope, *Conc. Magn. Reson.*, 1993, **5**, 43.
6 H. Rampel and J. M. Pope, *Conc. Magn. Reson.*, 1993, **5**, 43.
7 K. Wüthrich, *NMR of Proteins and Nucleic Acids*, New York, Wiley, 1986.
8 E. MacNamara, T. Hou, G. Fisher, S. Williams and D. Raftery, *Anal. Chim. Acta*, 1999, **397**, 9.
9 D. L. Olson, T. L. Peck, A. G. Webb, R. L. Magin and J. V. Sweedler, *Science*, 1995, **270**, 5244.
10 J. A. Rogers, R. J. Jackman, G. M. Whitesides, D. L. Olson and J. V. Sweedler, *Appl. Phys. Lett.*, 1997, **70**, 2464.
11 D. Rugar, R. Budakian, H. J. Mamin and B. W. Chui, *Nature*, 2004, **430**, 329.
12 A. Abragham, *Principles of Nuclear Magnetism*, Oxford, Oxford Univesity Press, 1961.
13 D. I. Hoult and R. E. Richards, *J. Magn. Reson.*, 1976, **24**, 71.
14 C. Massin, F. Vincent, A. Homsy, K. Ehrmann, G. Boero, P.-A. Besse, A. Daridon, E. Verpoorte, N. F. de Rooij and R. S. Popovic, *J. Magn. Reson.*, 2003, **164**, 242.
15 H. Wensink, F. Benito-Lopez, D. C. Hermes, W. Verboom, H. J. G. E. Gardeniers, D. N. Reinhoudt and A. Van Den Berg, *Lab Chip*, 2005, **5**, 280.
16 J. D. Trumbull, I. K. Glasgow, D. J. Beebe and R. L. Magin, *IEEE Trans. Biomed. Eng.*, 2000, **47**, 3.
17 K. Ehrmann, K. Pataky, M. Stettler, F. M. Wurm, J. Brugger, P.-A. Besse and R. Popovic, *Lab Chip*, 2007, **7**, 381.
18 Y. Maguire, I. L. Chuang, S. Zhang and N. Gershenfeld, *Proc. Natl. Acad. Sci. U. S. A.*, 2007, **104**, 9198.
19 K. Ehrmann, M. Gersbach, P. Pascoal, F. Vincent, C. Massin, D. Stamou, P.-A. Besse, H. Vogul and R. S. Popovic, *J. Magn. Reson.*, 2006, **178**, 96.
20 P. T. Callaghan, *Principles of Nuclear Magnetic Resonance Microscopy*, Oxford University Press, Oxford, 1991.
21 S. Ahola, F. Casanova, J. Perlo, K. Munnemann, B. Blumich and S. Stapf, *Lab Chip*, 2006, **6**, 90.
22 B. S. Akpa, S. M. Matthews, A. J. Sederman, K. Yunus, A. C. Fisher, M. L. Johns and L. F. Gladden, *Anal. Chem.*, 2007, **79**, 6128.
23 A. J. Moule, M. M. Spence, S. I. Hans, J. A. Seeley, K. L. Pierce, S. Saxena and A. Pines, *Proc. Natl. Acad. Sci. USA*, 2003, **100**, 9122.
24 J. Granwehr, E. Harel, S. Hans, S. Garcia, A. Pines, P. N. Sen and Y. Q. Song, *Phys. Rev. Lett.*, 2005, **95**, 075503.
25 E. Harel, C. Hilty, K. Koen, E. E. McDonnell and A. Pines, *Phys. Rev. Lett.*, 2007, **98**, 017601.
26 E. Harel and A. Pines, *J. Magn. Reson.*, 2008, **193**, 199–206.
27 S. Xu, V. V. Yashchuk, M. H. Donaldson, S. M. Rochester, D. Budker and A. Pines, *Proc. Natl. Acad. Sci. U. S. A.*, 2006, **103**, 12668.
28 L. Becerra, G. J. Gerfen, R. J. Temkin, D. J. Singel and R. G. Griffin, *Phys. Rev. Lett.*, 1993, **71**, 5361.